Special Contributions, Geophysical Institute, Kyoto University, No. 8, 1968, 31-44

A NUMERICAL INVESTIGATION OF HYDRODYNAMIC INSTABILITY OF A SHEAR FLOW IN A THERMALLY UNSTABLE FLUID LAYER

By

Tomio ASAI and Isao NAKASUJI

(Received October 30, 1968)

Abstract

The stability characteristics of a shear flow in an unstable stratified fluid layer is investigated based upon a finite difference approximation of the linearized Boussinesq equation system. The feasibility of numerical calculation is tested with the aid of the convection theory established by Rayleigh which yields the exact solution. Since the result obtained is satisfactory, the procedure is applied to the thermal convection in a Couette flow. It is found from the calculation that constant shear has the effect which suppresses development of the thermal convection. This effect of shear is striking for a convection cell of short wave length and decreases as a wave length of the convection cell increases. The convection cell which is long in the direction perpendicular to the basic flow suffers severely the prohibitive effect of the shear, while this effect decreases as the convection cell becomes longer in the direction parallel to the basic flow.

1. Introduction

Bénard [1900] demonstrated his experimental result on the onset of thermal instability in fluids, that is, a certain critical adverse temperature gradient must be exceeded before instability can set in and the motions which ensue on surpassing the critical temperature gradient have a stationary cellular character. Since then a number of investigations have been made both experimentally and theoretically. Among other things Rayleigh [1916] established a theoretical foundation for the Bénard convection mentioned above. On the basis of the theory of perturbation Rayleigh showed that instability must set in when the non-dimensional parameter R_a, referred to as the Rayleigh number later on, exceeds a certain critical value R_c and that when R_a just exceeds R_c, a stationary pattern of motions must come to prevail. Rayleigh's work has been extended to many different cases by Jeffreys [1926] and others. As is known well, the critical Rayleigh number predicted theoretically is quite well coincident with the one obtained experimentally (e. g., Schmidt and Milverton [1935]).

On the other hand some experiments of thermal instability in a shear

flow were performed by Graham [1933] and Chandra [1938]. They found that when a vertical shear is introduced into a fluid layer the chamber is filled with transverse rolls perpendicular to the direction of the flow and when the shear is increased the transverse rolls are replaced by longitudinal ones which are directed along the flow. The theoretical study of hydrodynamic stability of a stratified Couette flow was made by Taylor [1931], Case [1960], Dyson [1960] and others. They enunciated that a Couette flow with a stable stratification is hydrodynamically stable. The theory was extended to a Couette flow in an unstably stratified fluid layer by Kuo [1963]. He described the stability characteristics of the perturbations in terms of the Richardson number and the wave-number of the perturbation for the non-dissipative system.

In this paper we deal with the perturbation equations in a more general form which contain the terms of friction and heat conduction. Since it is difficult to solve these perturbation equations analytically, a numerical method is presented with use of a finite-difference approximation and is applied to study a thermal instability in the both types of flow with and without a shear. It is suggested that this method is applicable for investigating hydrodynamic instability of a flow with a thermal stratification which may not be analytically tractable.

2. Fundamental equations

We consider a perturbation in a horizontal layer of fluid of depth h which is confined between two parrallel horizontal planes at $z=0$ and $z=h$. As is shown in Fig. 1, in the undisturbed state the temperature $\bar{T}$ is constant over a horizontal plane and decreases linearly with z, while the velocity of basic flow $\bar{u}$ is horizontally unifrom and increases linearly with z, i. e.,

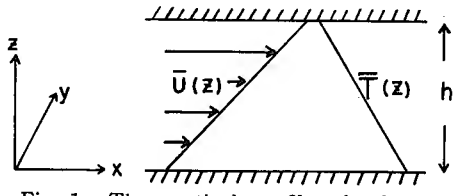

Fig. 1. The vertical profile of velocity and temperature for the basic field and the coordinate system.

$$\bar{T}=T_0-\Gamma z, \tag{2.1}$$

$$\bar{u}=u_0+\Lambda z. \tag{2.2}$$

Here $\Gamma=-\frac{d\bar{T}}{dz}$ is the constant lapse rate of the temperature and $\Lambda=\frac{d\bar{u}}{dz}$ is the constant vertical shear of the basic flow. Moreover T_0 and u_0 are the temperature and the velocity at $z=0$, respectively. The relation between the temperature T and the density ρ is given by

$$\rho=\rho_0\{1+\alpha(T_0-T)\}, \tag{2.3}$$

where ρ_0 is the density corresponding to the temperature T_0 and α is the thermal expansion coefficient.

On making use of the Boussinesq approximation, the equations of motion, the thermal energy equation and the continuity equation may be written as

$$\frac{\partial u'}{\partial t}+\bar{u}\frac{\partial u'}{\partial x}+\Lambda w'=-\frac{1}{\rho_0}\frac{\partial p'}{\partial x}+\nu\nabla^2 u', \tag{2.4}$$

$$\frac{\partial v'}{\partial t}+\bar{u}\frac{\partial v'}{\partial x}=-\frac{1}{\rho_0}\frac{\partial p'}{\partial y}+\nu\nabla^2 v', \tag{2.5}$$

$$\frac{\partial w'}{\partial t}+\bar{u}\frac{\partial w'}{\partial x}=-\frac{1}{\rho_0}\frac{\partial p'}{\partial z}+g\alpha T'+\nu\nabla^2 w', \tag{2.6}$$

$$\frac{\partial T'}{\partial t}+\bar{u}\frac{\partial T'}{\partial x}-\Gamma w'=\kappa\nabla^2 T', \tag{2.7}$$

$$\frac{\partial u'}{\partial x}+\frac{\partial v'}{\partial y}+\frac{\partial w'}{\partial z}=0, \tag{2.8}$$

where u', v' and w' are the velocity components of the perturbation in the x, y and z-direction. The x-axis is taken to be parallel to the basic flow $\bar{u}$. Del notation ∇ is the three-dimensional gradient operator, g is the acceleration due to gravitational force, p' is the departure of pressure from the hydrostatic pressure $\bar{P}(z)$, T' is the departure of temperature from the horizontal average $\bar{T}(z)$, ν is the coefficient of kinematic viscosity and κ is the coefficient of thermometric conductivity.

Differentiating (2.4) with respect to x and (2.5) with respect to y and adding, we obtain

$$\left(\frac{\partial}{\partial t}+\bar{u}\frac{\partial}{\partial x}-\nu\nabla^2\right)\frac{\partial w'}{\partial z}-\Lambda\frac{\partial w'}{\partial x}=\frac{1}{\rho_0}\nabla_H^2 p' \tag{2.9}$$

by making use of (2.8) and $\nabla_H^2=\frac{\partial^2}{\partial x^2}+\frac{\partial^2}{\partial y^2}$. Applying ∇_H^2 to (2.6) and differentiating (2.9) with respect to z and then eliminating p' from the resulting equations, we obtain

$$\left(\frac{\partial}{\partial t}+\bar{u}\frac{\partial}{\partial x}-\nu\nabla^2\right)\nabla^2 w'=g\alpha\nabla_H^2 T'. \tag{2.10}$$

Rewriting (2.7),

$$\left(\frac{\partial}{\partial t}+\bar{u}\frac{\partial}{\partial x}-\kappa\nabla^2\right)T'=\Gamma w'. \tag{2.11}$$

The equations (2.10) and (2.11) are the two final equations for w' and T', from which either one of the variables could be eliminated.

At the top and the bottom boundaries of the layer under consideration is assumed neither the normal component of the velocity nor the tangential stress. Therefore

$$w'=\frac{\partial^2 w'}{\partial z^2}=0 \qquad \text{at } z=0 \text{ and } h \tag{2.12}$$

with the aid of the continuity equation (2.8). In addition, the constant temperature are assumed to be maintained at both the boundaries:

$$T'=0 \qquad \text{at } z=0 \text{ and } h. \tag{2.13}$$

Now we take solutions of the form

$$\left.\begin{aligned} w' &= W(z)exp\{\mathrm{i}(k_x x+k_y y)+\sigma t\}, \\ T' &= \Theta(z)exp\{i(k_x x+k_y y)+\sigma t\}. \end{aligned}\right\} \tag{2.14}$$

Substituting (2.14) into (2.10) and (2.11), we obtain the ordinary differential equations for W and Θ with respect to z as follows:

$$\left\{\sigma+ik_x\bar{u}-\nu\left(\frac{d^2}{dz^2}-k^2\right)\right\}\left(\frac{d^2}{dz^2}-k^2\right)W+g\alpha k^2\Theta=0, \tag{2.15}$$

$$\Gamma W-\left\{\sigma+ik_x\bar{u}-\kappa\left(\frac{d^2}{dz^2}-k^2\right)\right\}\Theta=0, \tag{2.16}$$

where $k^2=k_x^2+k_y^2$.

Let us define the following non-dimensional quantities denoted by the superscript $*$

$$\left.\begin{aligned} \sigma &= \sigma^*\nu h^{-2}, \\ \bar{u} &= \bar{u}^*\Lambda h, \\ \Lambda &= \Lambda^*\nu h^{-2}, \\ k_x &= k_x^* h^{-1}, \\ k &= k^* h^{-1}, \\ z &= z^* h, \\ W &= W^*\nu h^{-1}, \\ \Theta &= \Theta^*\Gamma h. \end{aligned}\right\} \tag{2.17}$$

Substituting (2.17) into (2.15) and (2.16) and arranging the resulting equations, we obtain

$$\left\{\sigma^*+ik_x\Lambda^*\bar{u}^*-\left(\frac{d^2}{dz^{*2}}-k^{*2}\right)\right\}\left(\frac{d^2}{dz^{*2}}-k^{*2}\right)W^*+P_r^{-1}R_a k^{*2}\Theta^*=0, \tag{2.18}$$

$$-W^*+\left\{\sigma^*+ik_x^*\Lambda^*\bar{u}^*-P_r^{-1}\left(\frac{d^2}{dz^{*2}}-k^{*2}\right)\right\}\Theta^*=0, \tag{2.19}$$

where R_a is the Rayleigh number and P_r is the Prandtl number. These non-dimensional numbers are defined as

$$R_a=\frac{g\alpha\Gamma h^4}{\kappa\nu}, \qquad P_r=\frac{\nu}{\kappa}.$$

In addition, the Richardson number defined by $R_i=g\alpha\Gamma/\Lambda^2$ will be conveniently

introduced. It may be noted here that $\Lambda^*=(R_a/P_rR_i)^{1/2}$. The boundary conditions (2.12) and (2.13) are also replaced by

$$W^*=\frac{d^2W^*}{dz^{*2}}=0 \qquad \text{at } z^*=0 \text{ and } 1, \tag{2.20}$$

$$\Theta^*=0 \qquad \text{at } z^*=0 \text{ and } 1. \tag{2.21}$$

The set of the equations (2.18) and (2.19) is to be solved for W^* and Θ^*, subject to the boundary conditions (2.20) and (2.21) for given Rayleigh number and Richardson number.

3. Finite difference version

The set of linear differential equations (2.18) and (2.19) may now be transformed to a system of algebraic equations by approximating the derivatives of W^* and Θ^* by finite differences. The fluid layer will be divided vertically into n sublayers, each of which has thickness Δz with the adjacent levels designated from 0 at the bottom to n at the top of the fluid layer (see Fig. 2).

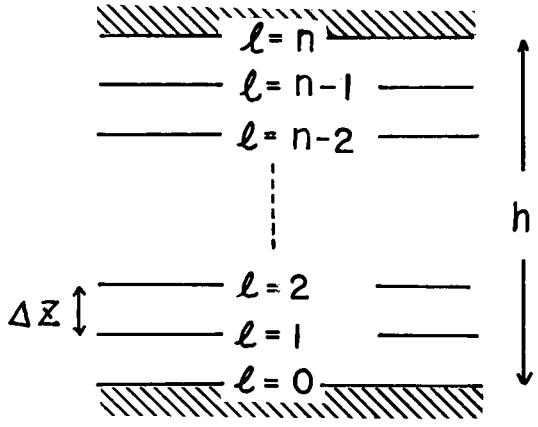

Fig. 2. A schematic representation of the n-layer model.

Use of the centered difference approximations for the derivatives in (2.18) and (2.19) at the l th level results in the following system of homogeneous algebraic equations:

$$-n^4W_{l-2}^*+C_lW_{l-1}^*-D_lW_l^*+C_lW_{l+1}^*-n^4W_{l+2}^*+k^{*2}P_r^{-1}R_a\Theta_l^*=0, \tag{3.1}$$

$$W_l^*+n^2P_r^{-1}\Theta_{l-1}^*-E_l\Theta_l^*+n^2P_r^{-1}\Theta_{l+1}^*=0, \tag{3.2}$$

where

$$C_l=in^2k_x^*\Lambda^*\bar{u}_l^*+4n^4+2n^2k^{*2}+n^2\sigma^*,$$

$$D_l=ik_x^*\Lambda^*\bar{u}_l^*(2n^2+k^{*2})+6n^4+4n^2k^{*2}+k^{*4}+\sigma^*(2n^2+k^{*2}),$$

$$E_l=ik_x^*\Lambda^*\bar{u}_l^*+P_r^{-1}(2n^2+k^{*2})+\sigma^*.$$

The variables W_l^* and Θ_l^* denote those at the l th level, respectively.

The conditions at the upper and the lower boundaries (2.20) and (2.21) are reduced to

$$\left.\begin{aligned} &W_0^*=W_n^*=0,\\ &W^*_{-1}+W_1^*=0,\\ &W_{n-1}^*+W_{n+1}^*=0, \end{aligned}\right\} \tag{3.3}$$

and

$$\Theta_0^*=\Theta_n^*=0. \tag{3.4}$$

The system of finite difference equations (3.1) and (3.2) brings about a set of simultaneous linear equations in $2(n-1)$ unknown variables, that is W_l^* and Θ_l^* at $l=1, 2, \cdots\cdots, n-1$. We can represent the set symbolically in the following matrix :

$$(A-\sigma^*B)X=0, \tag{3.5}$$

where X is the vector of the eigenfunction solution for W^* and Θ^*, and A and B are matrices with complex elements. Multiplying (3.5) by the inverse of B, we obtain

$$(B^{-1}A-\sigma^*I)X=0, \tag{3.6}$$

where I is the unit matrix and B^{-1} is the inverse of B. Provided that X is to be non-zero solution, the determinant of matrix $(B^{-1}A-\sigma^*I)$ must vanish, i. e.,

$$|B^{-1}A-\sigma^*I|=0 \tag{3.7}$$

This yields the so-called frequency equation for the frequency σ^*, the value of which can be calculated for given basic state of the fluid layer and wave length of the perturbation superposed on it, etc. Note that real value of σ^* does not signify a frequency but an amplification rate of amplitude of perturbation. The eigenvector for W^* and Θ^* can be obtained, in turn, by use of the eigenvalue. Since we are concerned with the stability characteristics, the amplification rate σ^* will be primarily discussed in the present study. A series of computations were made for a nmber of different values of R_a, R_i, wave length and so forth.

4. Feasibility of numerical method

In order to estimate the accuracy of the numerical solution, it is convenient to test its performance on known analytic solutions. The results of several such tests are presented here to demonstrate quantitatively the truncation errors of a numerical model and the effects of varying the vertical resolution.

Let us consider one of the simplest cases in which inviscid and non-conducting fluid without a basic flow is assumed. Setting $\bar{u}=\nu=\kappa=0$ in (2.15) and (2.16) and eliminating Θ from the resulting equations, we obtain

$$\frac{d^2W}{dz^2}-q^2W=0, \tag{4.1}$$

where

$$q^2=k^2\left(1-\frac{g\alpha\Gamma}{\sigma^2}\right).$$

Making use of the boundary condition $W(0)=W(h)=0$, the solution of (4.1) may be expressed as follows:

$$W=A\sin\frac{m\pi}{h}z \qquad (m=1, 2, \cdots\cdots), \tag{4,2}$$

and

$$h^2q^2=-m^2\pi^2.$$

Fig. 3 shows the dependence of the amplification rate of perturbation upon the vertical mode denoted by m. For convenience the ordinate of Fig. 3 indicates σ' which corresponds to the amplification factor of the perturbation defined by

$$\sigma'=\frac{1}{g\alpha\Gamma}\sigma^2=\frac{1}{1-\frac{q^2h^2}{k^2h^2}}. \tag{4.3}$$

In this case $k^2h^2=1$ is assumed. As is seen in Fig. 3, the amplification rate decreases rapidly with an increasing vertical mode of the perturbation denoted by m. In general, the number of roots obtained from the numerical model increases as the number of subdivision of a fundamental layer increases, since the order of the matrix increases with an increasing vertical indices. There is frequently an infinite number of eigenvalues associated with the analytic solution of a boundary value problem. Thus it would appear that increasing the number of subdivisions permits more roots to appear, particulary as additional nodal points. It is evident from Fig. 3 that the lowest mode $m=1$ is one which maximizes the amplification rate. This provides one of the causes by which numerical method adopoted here is made feasible.

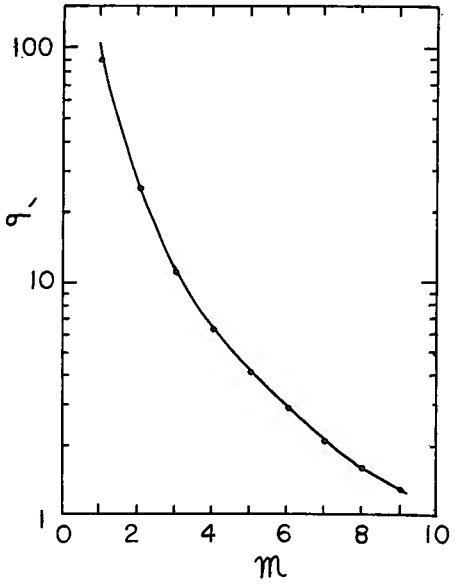

Fig. 3. The dependence of the amplification factor σ' on the vertical mode m.

Fig. 4 shows that the accuracy of

the amplification rate calculated by the numerical method varies with the number of sublayers for different values of vertical mode m. The relative error of the numerical solution is taken in the ordinate in units of per cent and the number of sublayers is in the abscissa. A solid line indicates variation of accuracy with the number of sublayers for the respective vertical mode of perturbation. Apparently numerical solution for each mode monotonically approaches to its exact one as the number of sublayers increases, while an increase of the number of sublayers yields an increased number of higher modes with lower accuracy. As far as the lowest mode is concerned, we can expect to obtain a considerably accurate solution using rather a small number of subdivisions of a fluid layer.

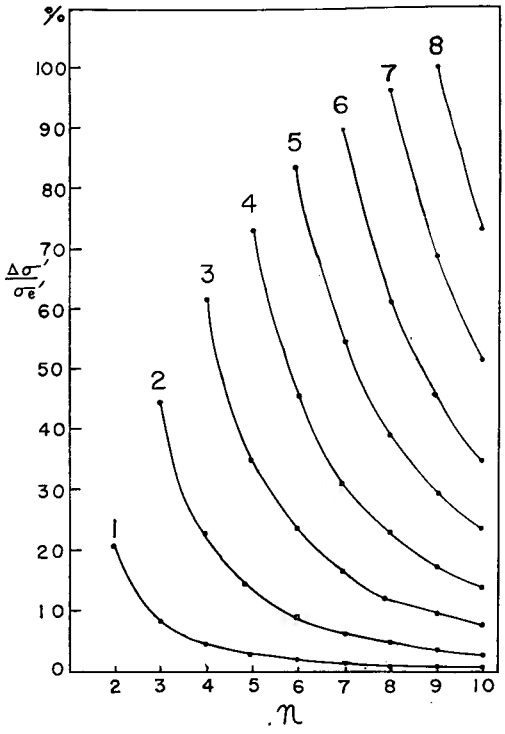

Fig. 4. The dependence of relative error $\Delta\sigma'/\sigma_e'$ of the amplification factor calculated by the numerical method on the number of sublayers for various values of vertical mode m. The number added to each curve denotes the value of the vertical mode m.

5. Results

(1) *No basic flow*

Prior to proceeding to the discussion of the thermal convection in a shear flow, we will consider Bénard cell convection in a viscous fluid layer in the absence of a basic flow. Assuming $\bar{u}=0$ in (2.15) and (2.16), we obtain the same equations as derived by Rayleigh [1916]. Therefore the results based on the numerical method may be compared with those obtained by Rayleigh. The values of the critical Rayleigh number R_c calculated by the numerical method are plotted for different numbers of sublayers in Fig. 5. As is seen in Fig. 5, the calculated value of R_c tends to approach the exact one, that is $R_c=657.5$, as the number of sublayers increases. For instance, when the number of sublayers is 8, the calculated value of R_c is 641 which results in the relative error of about 2.5 per cent. Fig. 6 shows that the relative error

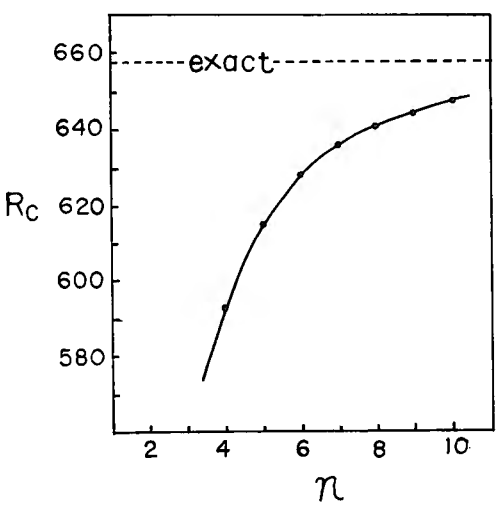

Fig. 5. Variation of critical Rayleigh number R_c calculated by the numerical method using the number of sublayers. The solid line represents the one obtained numerically and the broken line represents the one obtained from the exact solution.

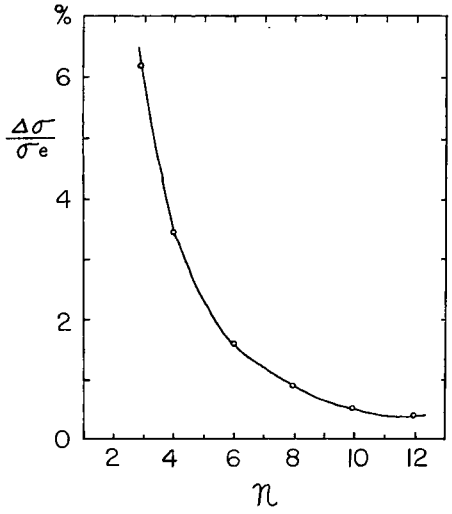

Fig. 6. Variation of relative error $\Delta\sigma/\sigma_e$ of the amplification rate calculated by the numerical method with the number of sublayers in the absence of basic flow.

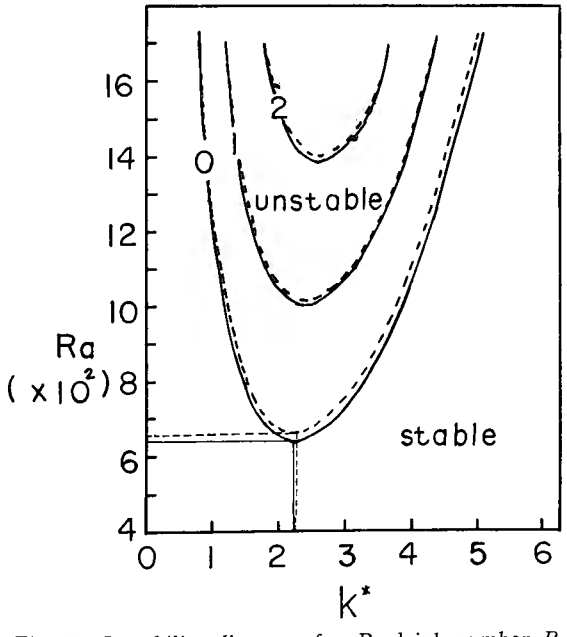

Fig. 7. Instability diagram for Rayleigh number R_a and dimensionless wave-number k^*. Solid lines and broken lines are isopleths of dimensionless amplification rates obtained from the numerical method and the exact solution respectively.

of the amplification rate of perturbation decreases with an increasing number of sublayers. An inspection of Fig. 6 indicates that the relative error may be less than 1 per cent for the multi-layer model subdivided into more than seven. Additional accuracy, if required, could be obtained by increasing the number of sublayers. The eight-layer representation will be employed in the following.

Now we shall examine the stability characteristics of perturbations which are obtained by making use of numerical method. Fig. 7 shows dependence of the amplification rate of perturbation on the non-dimensional wave-number and the Rayleigh number. Solid lines are the isopleths for different values of the amplification rate. The neutral curve labelled with 0 separates the unstable domain in the upper part of Fig. 7 from the stable one in the lower. The respective curves for the exact solution are represented by broken lines in Fig. 7. The calculated values of the amplification rate agree well with the exact ones. With regard to the critical Rayleigh number, it is indicated that the calculated value, 641, is a close approximation to the exact one, 657.5. The corresponding non-dimensional wave-numbers are 2.2 for both.

(2) *Basic flow with a constant vertical shear*

The investigation of primary concern to us deals with an influence of a vertical shear flow on a thermal convection. Since the Richardson number R_i is defined as the ratio of the static stability to the square of the vertical shear, the vertical shear can be measured by the Richardson number when the static stability is fixed to be constant. It is assumed that the Prandtl number $P_r=7$ which is nearly equal to the one for water at the standard state and $R_a=10^4$ in all calculations unless specifically stated otherwise.

Fig. 8 demonstrates variation of the amplification rate σ^* with the wave number k^* for different values of R_i. Here k_y/k_x is fixed as unity. As is seen in Fig. 8, a smaller value of R_i results in a smaller value of the amplification rate and in diminishing an unstable wave domain. The maximum of the amplification rate shifts toward a smaller wave-number by decreasing the value of R_i. As the value of R_i increases, the amplification rate curve tends to approach the one for $R_i=10^5$ which actually may be taken for the case without a shear. Moreover an inspection of Fig. 8 indicates that the amplification rate of an unstable perturbation is more seriously influenced by an increasing wave-number. This suggests that the vertical shear is more effective in suppressing a perturbation of shorter wave length.

Another characteristic of the perturbation will be discussed based on Fig. 9 in which the amplification rate versus the ratio between the wave-numbers in the x and the y directions k_y/k_x is illustrated for three different values of

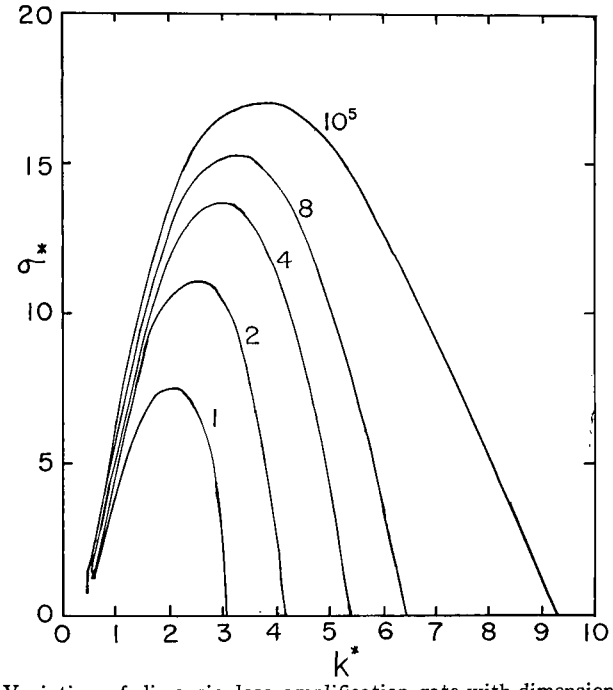

Fig. 8. Variation of dimensionless amplification rate with dimensionless wave-number k^* for various values of the Richardson number. The number added to each curve denotes the value of the Richardson number.

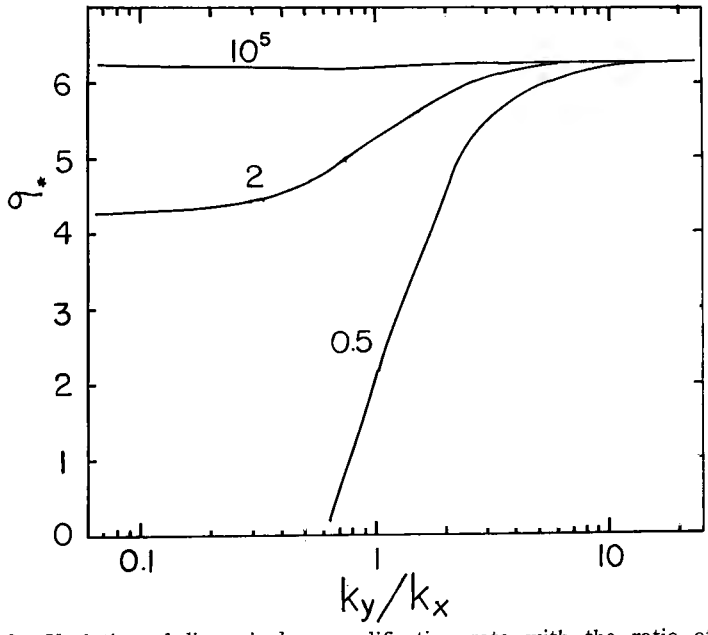

Fig. 9. Variation of dimensionless amplification rate with the ratio of the wave-number in the direction perpendicular to the basic flow to the one in the direction parallel to the basic flow. The number added to each curve denotes the value of the Richardson number.

R_i. Here k^* is fixed as unity. A decreasing value of R_i results in a reduction of the amplification rate of a perturbation with transverse mode for which $k_y/k_x \ll 1$. For instance, a perturbation of the ratio k_y/k_x less than 0.6 is unable to grow in the case of $R_i=0.5$. On the other hand no difference in the amplification rate can be found among the cases where there are different values for R_i for a large value of k_y/k_x. Since a small Richardson number corresponds to a large vertical shear of the basic flow, it is evident that the suppressing influence of vertical shear is effective in the transverse-mode perturbation while it is not effective in the longitudinal one. Thus it is implied that the longitudinal convection rolls favour occurrence in a thermally unstable fluid layer with a vertical shear. The implication agrees with the theoretical results obtained by Kuo [1963] and Asai [1964] and also with the experiments made by Graham [1933] and Chandra [1938] except in the case of a comparatively small shear where transverse rolls were observed.

Fig. 10 shows the dependence of the amplification rate of perturbations on the Richardson number R_i and the non-dimensional wave-number k^*. Again k_y/k_x is assumed to be unity. It is seen that the neutral curve labelled 0 shows

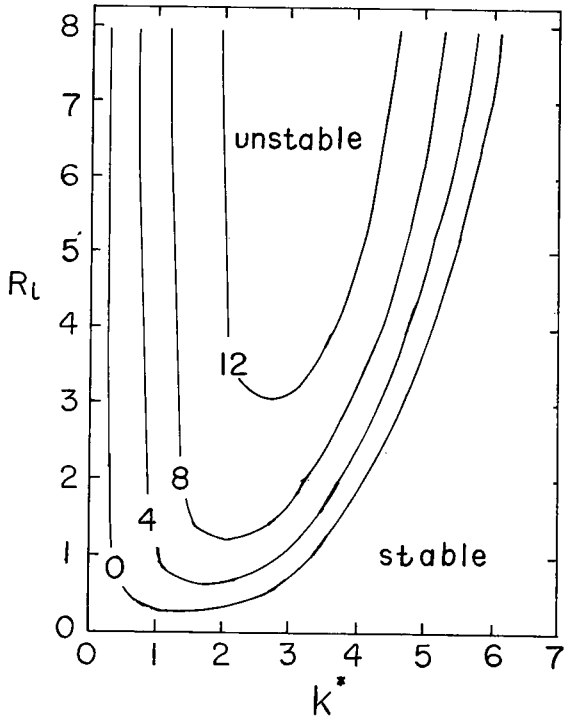

Fig. 10. Instability diagram for the Richardson number R_i and dimensionless wave-number k^*. The solid lines are isopleths of the dimensionless amplification rate.

two cut-off ends to instability, one at a small wave-number and the other at a large wave-number. Both of them are due primarily to a stabilization of viscosity and conductivity of the fluid. In addition it should be taken into consideration that the effect of a static instability diminishes at a smaller wave-number while a suppressing effect of a vertical shear increases at a larger wave-number. As is noticed in Fig. 10, the amplification rate of a small wave-number is almost independent of the Richardson number. In other words the perturbation of a small wave-number would be free from an effect of vertical shear. Thus the maximum amplification rate appears at 1.5~3.5 of the non-dimensional wave-number which shifts slightly toward its larger value with an increasing value of R_i. All the perturbations are stable where the value of R_i is less than about 0.25.

6. Conclusion

The stability characteristics of a constant shear flow in an unstably stratified fluid layer is studied by making use of the numerical solution for a linearized system of the Boussinesq equations. The results obtained above will be summarized in the following.

(1) The numerical method employed here provides the better approximation to the solution as the number of sublayers used for vertical finite-differencing is increased. A good accuracy is expected for perturbation of the lowest mode, which would play an essential role in the stability characteristics, even for a rather small number of subdivisions.

(2) In general a constant vertical shear of the basic flow exerts an influence on reducing development of a perturbation.

(3) A stabilization of the vertical shear is more effective in a perturbation of shorter wave length. Hence an appearance of the most unstable perturbation shifts toward a longer wave length with an increasing shear.

(4) The suppressing effect of the vertical shear is much more striking on a transverse perturbation when compared with a longitudinal one. This gives a preference for the longitudinal convection rolls in an atmosphere with a vertical shear.

Remarks

The Rayleigh number R_a has been fixed as 10^4 here. In this case we are able to find only one unstable wave which was examined in the preceding sections. In order to investigate the case with more unstable stratification we set a much larger value of R_a such as 10^5. There appeared multiple unstable waves which may be classified into two types. One is the unstable wave which travels at the mean velocity of the basic flow, while the others propagate at

a velocity different from the former. Therefore we must examine the details of structure and energy conversion of these unstable waves to clarify their dynamical features. Moreover, to study the hydrodynamic stability characteristics for an unstably stratified fluid layer in which the basic flow has an arbitrary velocity profile, we shall apply the numerical method employed here. We shall report the results of these findings in a separate paper.

Acknowledgments

The authors express their appreciation for the encouragement given by Prof. R. Yamamoto throughout the course of this study. Thanks are extended to Miss A. Nagasawa for her assistance.

Numerical calculations were made with the use of KDC-II of the Computation Center and IBM-360 of the Japan IBM Co. in Osaka. This work has been financially supported by Funds for Scientific Research from the Ministry of Education.

References

Asai, T., 1964; Cumulus convection in the atmosphere with vertical wind shear: Numerical experiment, J. Meteor. Soc. Japan, 42, 245–259.

Bénard, H., 1900; Les tourbillons cellulaires dans une nappe liquide, Rev. gén. Sci. pur. appl., 11, 1261–1271, 1309–1328.

Case, K. M., 1960; Stability of inviscid plane Couette flow, Phys. Fluids, 3, 143–148.

Chandra, K., 1938; Instability of fluids heated from below, Proc. Roy. Soc., A 164, 231–242.

Dyson, F. J., 1960; Stability of an idealized atmosphere, II, Zeros of the confluent hypergeometric function, Phys. Fluids, 3, 155–157.

Graham, A., 1933; Shear patterns in an unstable layer of air, Phil. Trans. Roy. Soc., 232, A 714, 285–296.

Jeffreys, H., 1926; The stability of a layer of fluid heated below, Phil. Mag., 2, 832–844.

Kuo, H. L,, 1963; Perturbations of plane Couette flow in stratified fluid and origin of cloud streets. Phys. Fluids, 6, 195–211.

Rayleigh, L., 1916; On convective currents in a horizontal layer of fluid when the higher temperature is on the under side. Phil. Mag., 32, 529–546.

Schmidt, R. J. and S. W. Milverton, 1935; On the instability of a fluid when heated from below, Proc. Roy. Soc., A 152, 586–594.

Taylor, G. I., 1931; Effect of variation in density on the stability of superposed streams of fluid, Proc. Roy. Soc., A 132, 499–523.